Nano World Journal

https://doi.org/10.17756/nwj.2023-s1-059

Research Article

Open Access

Numerical Analysis of Thermo-fluid Properties Inside a Food Processing Unit

Shubham Kumar[1], Prabhat Shahi[1], Savyasachi Chaubey[1], Saddam Hossain Mullick[2] and Pranab Kumar Kundu[1*]

[1]MNNIT Allahabad, Prayagraj, Uttar Pradesh, India
[2]National Institute of Technology Sikkim, Ravangla, South Sikkim, Sikkim, India

***Correspondence to:**
Pranab Kumar Kundu
MNNIT Allahabad, Prayagraj,
Uttar Pradesh, India.
E-mail: pranabkundu@gmail.com;
pranabk@mnnit.ac.in

Received: November 24, 2022
Accepted: April 17, 2023
Published: April 19, 2023

Citation: Kumar S, Shahi P, Chaubey S, Mullick SH, Kundu PK. 2023. Numerical Analysis of Thermo-fluid Properties Inside a Food Processing Unit. *NanoWorld J* 9(S1): S302-S307.

Published by United Scientific Group

Abstract

Food products are continuously subjected to heating and cooling in a processing unit. This thermal treatment is expected to be unaltered throughout the volume in order to ensure the quality of the food as well as giving them optimum temperature for storage without deterioration. Thermo-fluid analysis has been performed theoretically on a food processing unit, considering it to be trapezoidal in shape with a horizontal porous partition in between. The bottom wall is subjected to a uniform temperature heating whereas the top wall is shielded, and the two inclined adjacent walls are sustained at a relatively low temperature. The different thermo-fluid properties like isothermal and stream function patterns, irreversibility generations are observed under the variation of Rayleigh number ($10^3 \leq Ra \leq 10^5$). The circulation has been found to increase with the increase in the Rayleigh number. The partition shows an imperative role in the distribution of heat throughout the cavity.

Keywords

Rayleigh number, Stream functions, Isotherms, Non-uniform heating

Nomenclature

H is Height of the enclosure, m; k is Thermal conductivity, $Wm^{-1}K^{-1}$; P is Non-dimensional pressure component; U is Dimensionless velocity component along x; V is Dimensionless velocity component along y; α is Thermal diffusivity, m^2s^{-1}; β is Volumetric expansion coefficient, K^{-1}; T is Temperature of the fluid, K; g is Gravitational acceleration, ms^{-2}; Da is Darcy number; c_p is Specific heat at constant pressure, $Jkg^{-1}K^{-1}$; θ is Dimensionless temperature; Ra is Rayleigh number; Pr is Prandtl number; Nu is Nusselt number; ρ is Density of fluid, kgm^{-3}; υ is Kinetic viscosity, m^2s^{-1}; ψ is Irreversibility distribution ratio; S is Entropy generation.

Introduction

Buoyancy driven convection form of heat transfers has many application fields such as nuclear core reactor, electronic thermal management systems, heating and ventilation systems, boilers, food processing units, etc. [1-5]. There has been much research with respect to study of natural convection inside the enclosures with different geometries [6-15]. Mullick et al. [1, 3, 10-14] have reported natural convection inside the enclosures with the applications of non-uniform temperature from below or top. They have varied *Ra*, periodic length and *Da*, and concluded that heat transfer rate significantly enhances with *Ra* and *Da*. They also have observed that the heat transfer rate declines with the lessen in periodic length inside an enclosure. Corcione [16] has shown the distribution of thermal energy and fluid flow due to free convection in rectangular cavities where

the heat source is pointed out from below and cooled from above. They have varied *Ra* (10^3 to 10^6), aspect ratio (0.66 to 8), and thermal conditions of the vertical wall and reported that the heat transfer significantly enhances when zero heat flux vertical wall is replaced by a cooler wall. Basak et al. [17] have also contributed by working on the study of free convection in a cavity having square contour whose bottom wall is heated both homogenously and sinusoidally while the sideways walls are preserved at a relatively low temperature and the top wall is insulated. They have observed the heat transit behaviour with the change in *Ra* (10^3 to 10^5) and *Pr* (0.7 to 10). They have found maximum heat transfer rate at the center for homogeneous heating whereas the heat transit is more near the corner of the bottom wall for sinusoidal heating. Akterian and Fikinn [18] have conducted a study on numerical simulation on any arbitrary shaped canned foods to predict the heat transfer rate inside it, during the sterilization process. This study analyses heat transit by diffusion in food processing industries. They have also proposed a model where a detailed study of unsteady conduction is analyzed during the preparation of canned food under different boundary conditions. Paroncini and Corvaro [19] have conducted the study of free convection in a square shaped enclosure with the placement of heat source inside the cavity, both numerically and experimentally. Their results of experimental work are in reasonably match with the numerical study which can help to elaborate the work for higher *Ra*. They have shown that average *Nu* enhances with *Ra*. Chen and Chen [20] and Cianfrini et al. [21] have studied the mechanism with partially heated sources in vertical square and tilted square enclosures, respectively. They have observed that average *Nu* enhances with *Ra*. A study which involves the SIMPLER algorithm to illuminate the momentum, mass and energy equations for a specific model of rectangular enclosure with air medium has been performed by Corcione and Habib [22]. They have varied *Ra* (10^3 to 10^7), *Pr* (0.7 to 700), and tilting angle (-75° to 75°), and concluded that heat transfer rate enhances with *Ra*, *Pr*, and size of the heat source. Heat transit behaviour significantly depends on the shape and orientation of an enclosure. A study has been performed by Varol et al. [23] which involves varying parameters such as tilt angle of 2D geometry from square to trapezoid, fluid porous medium, and cooling and heating from different walls. Three different positions of the cooler are defined for their work with the change in *Ra* and aspect ratio. The position of the cooler helps to modify the heat transfer rate.

The majority of research works which have been carried out in this field are with regular shaped enclosures. Based on the available literature, it can be observed that there are no such studies available where natural convection inside trapezoidal enclosure with porous partition in-between has been performed in order to explore its suitability for the food processing units. Heating is pragmatic from the lowermost wall while the top wall is insulated, and the left/right inclined walls are kept relatively cold. In the present problem of the analysis of food processing unit, a trapezoidal cavity with a horizontal porous partition has been considered to observe the thermo-fluid behaviors inside it. The performance of the present system has been evaluated under different bottom wall heating conditions. Stream function, isotherm patterns, and entropy generation have been estimated for the present system to reach conclusions.

Problem Definition and Mathematical Modeling

In order to simplify the study, few assumptions are made. The flow is supposed to be laminar, 2D, and incompressible in nature. The fluid is considered to be Newtonian in nature, with the properties remaining unaltered except the density variation in the y-momentum equation, which is estimated based on the Boussinesq approximation. Figure 1 illustrates the problem domain.

In the single-domain tactic, the identical conditions at the fluid/porous interface are implicitly ensured, and thus the implementation of the numerical scheme is simplified. The governing differential equations of the two domains can be combined by introducing a binary parameter, which is given by:

$$X_p(x,y)=\begin{cases}1 & \text{if in porous region}\\ 0 & \text{if in fluid region}\end{cases}$$

The dimensionless governing equations yield the following forms [10, 24-29].

$$\text{Continuity: } \frac{\partial U}{\partial \xi}+\frac{\partial V}{\partial \eta}=0 \tag{1}$$

$$\text{x-mom: } (1-X_p)\left(U\frac{\partial U}{\partial \xi}+V\frac{\partial U}{\partial \eta}\right)=-\frac{\partial P}{\partial \eta}+Pr\left(\frac{\partial^2 U}{\partial \xi^2}+V\frac{\partial^2 U}{\partial \eta^2}\right)-\left(\frac{Pr}{Da}+\frac{C}{Da^{\frac{1}{2}}}|U|\right)U \tag{2}$$

$$\text{y-mom: } (1-X_p)\left(U\frac{\partial V}{\partial \xi}+V\frac{\partial V}{\partial \eta}\right)=-\frac{\partial P}{\partial \eta}+Pr\left(\frac{\partial^2 V}{\partial \xi^2}+V\frac{\partial^2 V}{\partial \eta^2}\right)-X_p\left(\frac{Pr}{Da}+\frac{C}{Da^{\frac{1}{2}}}|V|\right)V+\text{RaPr} \tag{3}$$

$$\text{Energy: } U\frac{\partial \theta}{\partial \xi}+V\frac{\partial \theta}{\partial \eta}=\left(X_p\left(R_k-1\right)+1\right)\left(\frac{\partial^2 \theta}{\partial \xi^2}+\frac{\partial^2 \theta}{\partial \eta^2}\right) \tag{4}$$

For non-dimensionalization of the governing equations, the following schemes have been adopted.

$$\xi=\frac{x}{L},\ \eta=\frac{y}{L},\ U=\frac{uL}{\alpha},\ V=\frac{vL}{\alpha},\ \theta=\frac{T-T_C}{T_H-T_C},\ P=\frac{pL^2}{\rho\alpha^2}\ or\ \frac{p_D L^2}{\rho\alpha^2} \tag{5}$$

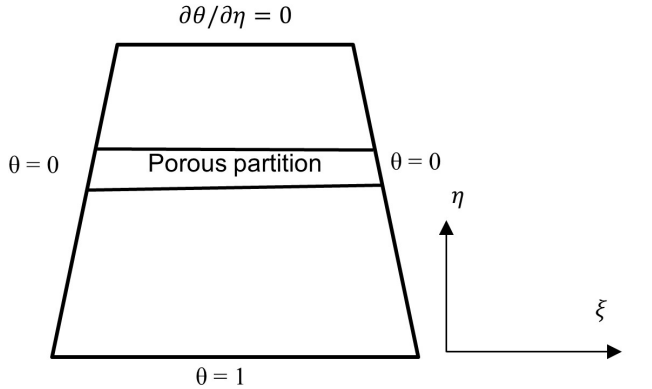

Figure 1: Schematic of the problem domain with boundary condition.

Where, $\alpha = \frac{k}{(\rho c_p)}$, thermal diffusivity;

$Ra = \frac{\rho g \beta (T_H - T_C) L^3}{\alpha \mu}$, Rayleigh number;

$Pr = \frac{\mu c_p}{k}$, Prandtl number;

$Da = \frac{K}{L^2}$, Darcy number

and $R_k = \frac{k_{eff}}{k}$, Thermal conductivity ratio.

Entropy generation inside the food processing unit can be estimated as below.

$$S = \left[\left(\frac{\partial \theta}{\partial X}\right)^2 + \left(\frac{\partial \theta}{\partial Y}\right)^2\right] + \left[\psi\left\{\left(U^2 + V^2\right) + Da\left(2\left[\left(\frac{\partial U}{\partial X}\right)^2 + \left(\frac{\partial V}{\partial Y}\right)^2\right] + \left(\frac{\partial U}{\partial Y} + \frac{\partial V}{\partial X}\right)^2\right)\right\}\right] \quad (6)$$

The non-dimensional boundary conditions at the different walls are stated next.

Upper wall: U = V = 0 and $\frac{\partial \theta}{\partial \eta} = 0$;

Lowermost wall: U = V = 0 and θ = 1;

Sideway walls: U = V = 0 and θ = 0.

Commercial software, Ansys Fluent has been employed in order to solve the governing equations through the finite volume approach during which energy, momentum and mass are conserved in each control volume as well as in the total domain. In the momentum equation, the velocity and the pressure terms are coupled together through SIMPLE algorithm, herein.

The code validation and grid independency study have been carried out for accurate prediction of thermal flow behavior inside the cavity. For validating the present code, results produced by the present code are compared with the existing works. For this, calculated average *Nu* along the conducting walls is compared with established works, which are depicted in table 1. From table 1, it can be concluded that the results are in significantly match the previous works, confirming the accuracy of the present code.

The mathematical inquiry has been also imperiled to the grid independency test to acquire the truthful solution. For grid independency study, the parameter conceived for the exertion is Ra = 10^5. The total entropy generation inside the cavity is calculated then for a piece refinement of grids and the results are compared with the preceding grid as depicted in table 2.

Table 1: Results for code validation study.

Sl No	Parameters selected for code validation	Existing results	Present results	% in change
1	*Da* = 10^{-3}, *Ra* = 10^5, and Φ = 0° [26]	2.623	2.610	0.38
2	*Ra* = 10^5, *Pr* = 10, and uniform heating [17]	8.61	8.58	0.34
3	*Da* = 10^{-1}, *Ra* = 10^5, and *Pr* = 1 [27]	4.385	4.276	2.4

The optimum nodes and elements selected for the current work are 23309 and 22900, respectively, to prevent grid dependency as from table 2, it can be observed that the entropy generation varies only 0.1 % for further grid refinement.

Table 2: Comparison results for grid independency test.

Sl No	Number of nodes	Number of elements	Total entropy generation	% in change of Total entropy generation
1	1538	1435	142.2	-
2	5935	5730	152.9	7.5
3	13192	12885	158.2	3.5
4	23309	22900	161.1	1.8
5	58966	58169	161.3	0.1

Results and Discussion

The chief objective of this study is to evaluate the detailed thermo-fluid characteristics inside a food processing unit heated from below while maintaining a constant temperature at the bottom wall. A trapezoidal enclosure with a horizontal porous partition having porosity 0.01 is conceived herein where the stream functions, isotherms and entropy generations are evaluated under different *Ra* values viz. 10^3, 10^4, and 10^5. The top wall has been insulated and both the inclined sidewalls are retained at a relatively cold temperature. The variations of thermo-fluid characteristics under different *Ra* values are observed and recorded in both the lower and upper parts of the enclosure as delineated subsequently.

Stream function and isotherm patterns

In order to enclounter the impact of *Ra* on energy transfer, three distinct values of *Ra* are ruminated, *Ra* = 10^3, *Ra* = 10^4, and *Ra* = 10^5, respectively, while *Pr* is sustained at a constant value of 0.7. Figure 2 illustrates the variation of stream function and isotherms with *Ra*. As the bottom wall is heated at higher constant temperature and the sidewalls are kept cold, the air starts to move up at the centre. It then moves towards the sidewalls and comes down to form two circulations, one clockwise and another anti-clockwise as can be seen from the stream function contours (left). The circulating air transfers the heat to the partition via convection and then a similar phenomenon takes place inside the above section. Therefore, total four circulations are noticed inisde the cavity. Strength of the circulation is more in lower part of the cavity while compared with the upper part of the enclosure irrespective of *Ra*. The values of stream fuction of upper portion is only 1.2 whereas in lower portion, this value is 6.3 (almost six times). This is due to the position of the heat source that provides heat directly to the bottom wall whereas heat transfers to upper portion through porous partition.

Natural convection is a strong function of *Ra*. In order to estimate the impact of *Ra* on the thermo-fluid properties inside the cavity, variations of isotherm and stream function patterns under different Ra during uniform heating are estimated and displayed in figure 2 at constant *Pr* (*Pr* = 0.7). It can be seen from figure 2 that the circulation strength is very less at the lower values of *Ra* (*Ra* = 10^3 and 10^4). This is due to the lower strength of buoyancy force that leads to conduction

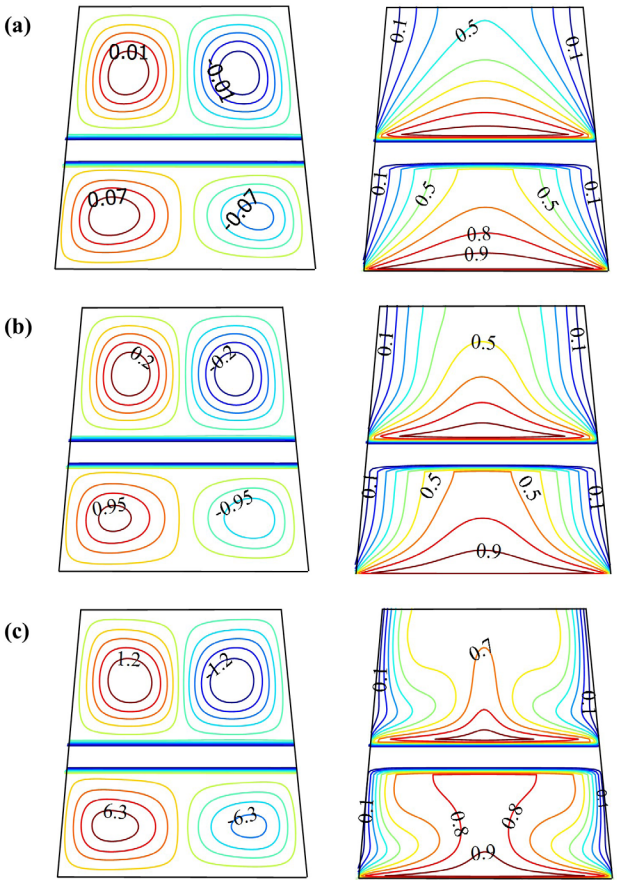

Figure 2: Contour of stream function and isotherms for *Ra* **(a)** 10^3, **(b)** 10^4, and **(c)** 10^5 at *Pr* = 0.7.

leading heat flow, which is also supported by the smooth natures of the isotherms. Non-dimensional temperature is smoothly disseminated from the conducting wall to the cavity, which signifies the diffusion leading energy transit throughout enclosure. Furthermore, it is found that the circulation strength drastically rises with the boost in *Ra* owing to significant augmentation of buoyancy force that prolongs the convection strength within the cavity as can be seen in figure 2b and 2c. From the isotherm patterns, it is also noticed that these bend toward the vertical wall indicating significant transfer of heat from hot bottom wall to cold vertical wall due to convection. For example, the strength of the circulation rolls is only 0.07 (lower cell) for $Ra = 10^3$, whereas the magnitude of the strength of the circulation roll is 6.3 for $Ra = 10^5$. Additionally, high strength circulation roll is found nearer to the core that tends to zero gradually towards the wall because of no slip boundary conditions.

It can be perceived that the isotherms are symmetric around the line passing through the mid-section of the bottom wall and are symmetrically distributed below towards the side walls. However, for smaller *Ra* the penetration of heat is low as can be seen in the figure as the isotherms approach the partition. It can be perceived (Figure 2b) that at $Ra = 10^5$, the circulation inside the trapezoidal enclosure (both above and below cavities) also intensifies as evident from the superior extents of the stream functions. Also, the buoyancy driven circulations are greater at the center of the cavities and lesser at the walls owing to no slip boundary conditions.

Entropy generation

In order to obtain more depth of heat transit characteristics inside the enclosure, entropy generation has been estimated and critically examined in this subsection. Figure 3 epitomizes the contour of local entropy production at different values of *Ra* for both heat transfer (left panel) and fluid friction (right panel) irreversibilities. From figure 3a, it can be detected that the entropy generation owing to fluid friction effect is very small and is present along the corners of the walls and the partition. With the increase in *Ra*, entropy generation attributable to both heat transfer and fluid friction also increases thus, irreversibility increases around the corners as can be perceived from figure 3b and 3c. However, it can be seen from figure 3 that around the partition, entropy generation near the bottom wall is quite high. This is attributable to the high temperature gradient between the cold and hot air. At low *Ra*, it can be noticed that the entropy production by reason of fluid friction is almost negligible while compared with the entropy production owing to the heat transfer. This shows conduction is more prevalent than convection. Further, with the rise in *Ra*, fluid friction irreversibility enhances more significantly as compared to heat transfer irreversibility. This is owing to the buoyancy actuated fluid flow inside the enclosure, which is drastically escalated with the increase in *Ra*. For example, heat transfer irreversibility enhances two times whereas fluid friction irreversibility enhances more than four hundred times for a change in *Ra* from 10^3 to 10^5.

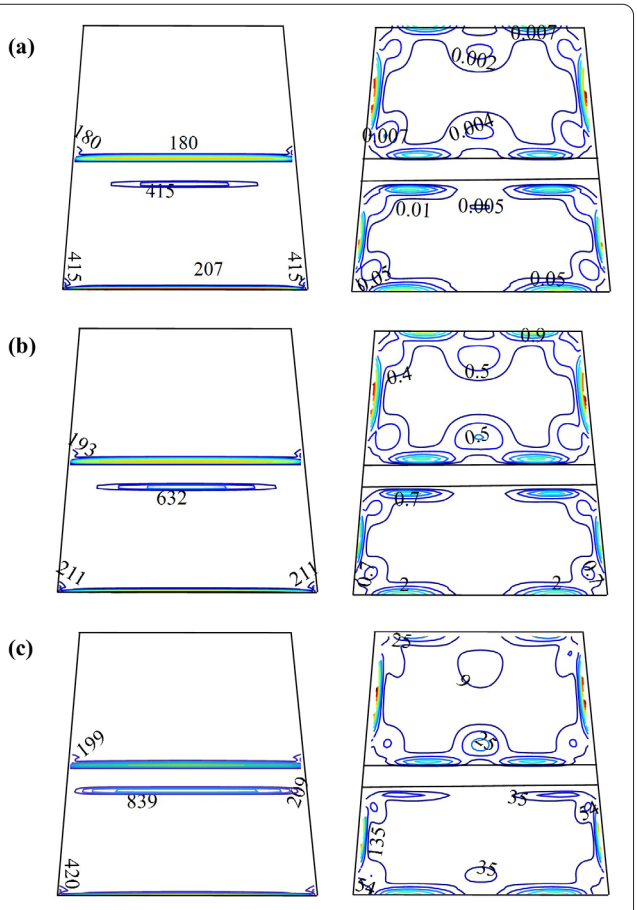

Figure 3: Contour of heat transfer irreversibility (left) and fluid friction irreversibility (right) for *Ra* **(a)** 10^3, **(b)** 10^4, and **(c)** 10^5 at *Pr* = 0.7.

Table 3 represents the distinction of total entropy production at different *Ra* values. At small *Ra*, heat transfer irreversibility is more whereas the fluid friction irreversibility is low as diffusion leading energy transit at the presence of lower buoyancy force takes place. With the increase in *Ra*, fluid friction irreversibility enhances drastically. Therefore, contribution of entropy production due to fluid friction is more prominent at high *Ra* whereas heat transfer irreversibility contribution is more at low *Ra*.

Table 3: Total entropy production.

Sl No	*Ra*	S_θ	S_ψ	S_T
1	10^3	63.21	0.007	63.21
2	10^4	65.53	0.99	66.51
3	10^5	73.05	87.09	160.14

After analyzing all the isotherm, stream-function and entropy generation plots it can be seen that it is suitable to choose a *Ra* such that the air circulation and heat distribution inside the enclosure is high while the entropy generation is admissible. Assuring these conditions, a food processing unit can ensure good quality products and optimized working conditions based on cost, time and material used. Total heat transfer irreversibility is very large at low *Ra* due to high temperature gradients. However, the total fluid friction irreversibility is very little at small *Ra* owing to less buoyancy force inside the cavity. Increment of total entropy because of heat transfer irreversibility is less as related to total fluid friction irreversibility. Again, this is due to buoyancy actuation with *Ra* which subsequently increases the total fluid friction irreversibility.

Conclusion

The prime aim of the present work is to study the impact of various *Ra* on the air circulation and temperature dispersal in a trapezoidal enclosure with a horizontal porous partition as a food processing unit. The succeeding decisions can be anecdotal from the present work.

- The circulation rate is very high for higher *Ra* (10^5).
- At low *Ra*, heat accumulation is comparatively higher at the bottom wall and with the increase in *Ra*, heat distribution increases at the sidewalls.
- The effect of presence of partition demonstrates that the temperature in the fluid above the partition is somewhat lower at low *Ra*, and uniform distribution of heat is observed for higher *Ra* values.
- Higher irreversibilities are observed at the corners of the enclosure and about the partition of the enclosure.

Acknowledgements

None.

Conflict of Interest

The authors declare no conflict of interests that are relevant to the content of this article.

Credit Author Statement

Shubham Kumar: Experimentation, Data analysis, Writing - original draft preparation; Prabhat Shahi: Writing - original draft preparation; Savyasachi Chaubey: Writing - original draft preparation; Saddam Hossain Mullick: Writing - original draft preparation; Pranab Kumar Kundu: Writing - review and editing, Supervision. All the authors read and approved the manuscript.

References

1. Mullick SH, Dasgupta, D, Kundu PK. 2022. Numerical study on natural convection and entropy generation inside a fluid saturated square porous enclosure with nonuniform heating from top. *J Porous Media* 25(1): 83-102. https://doi.org/10.1615/JPorMedia.2021039355
2. Mullick SH, Dasgupta D, Kundu PK. 2022. Numerical examination of natural convection and entropy formation inside air-saturated porous enclosure to create thermally active region with periodic heating/cooling. *J Porous Media* 25(9): 29-50. https://doi.org/10.1615/JPorMedia.2022042356
3. Mullick SH, Dasgupta D, Kundu PK. 2022. Influence of lower period of heating and high buoyancy inside fluid saturated porous enclosure on transient natural convection. *Sādhanā* 47(3): 149. https://doi.org/10.1007/s12046-022-01917-z
4. Mullick SH, Kumar A, Kundu PK. 2020. Numerical study of natural convection inside a square cavity with non-uniform heating from top. *J Inst Eng India Ser C* 101(6): 1043-1050. https://doi.org/10.1007/s40032-020-00618-y
5. Mullick SH, Dasgupta D, Kundu PK. 2021. Entropy generation inside a tilted air saturated porous quadratic enclosure. In Proceedings of the 48th national conference on fluid mechanics and fluid power. BITS Pilani, Pilani Campus, RJ, India.
6. Acharya S, Dash SK. 2017. Natural convection heat transfer from a short or long, solid or hollow horizontal cylinder suspended in air or placed on ground. *J Heat Transf* 139(7): 072501. https://doi.org/10.1115/1.4035919
7. Acharya S, Agrawal S, Dash SK. 2018. Numerical analysis of natural convection heat transfer from a vertical hollow cylinder suspended in air. *J Heat Transf* 140(5): 052501. https://doi.org/10.1115/1.4038478
8. Acharya S, Dash SK. 2021. Natural convection and entropy generation in a porous enclosure filled with non-Newtonian nanofluid. *J Thermophys Heat Transf* 35(3): 438-458. https://doi.org/10.2514/1.T6126
9. Acharya S, Dash SK. 2019. Natural convection in a cavity with undulated walls filled with water-based non-Newtonian power-law CuO–water nanofluid under the influence of the external magnetic field. *Numer Heat Transf Part A Appl* 76(7): 552-575. https://doi.org/10.1080/10407782.2019.1644898
10. Mullick SH, Dasgupta D, Kundu PK. 2022. Numerical investigation on natural convection inside closed cavity to create thermally active region with periodic heating/cooling. *J Therm Anal Calorim* 147: 13861-13878. https://doi.org/10.1007/s10973-022-11688-8
11. Mullick SH, Dasgupta D, Kundu PK. 2019. Transient heat transfer analysis during natural convection at high Ra number and small period of heating from bottom wall. In Proceedings of the 25th National and 3rd International ISHMT-ASTFE Heat and Mass Transfer Conference, pp 545-550. https://doi.org/10.1615/IHMTC-2019.920
12. Mullick SH, Dasgupta D, Kundu PK. 2021. Influence of central angle on buoyancy driven thermal flow behaviours inside a circular porous enclosure heating from below. In Proceedings of the 26th National and 4th International ISHMT-ASTFE Heat and Mass Transfer Conference. IIT Madras, Chennai, Tamil Nadu, India, pp 1101-1106. https://doi.org/10.1615/IHMTC-2021.1670
13. Mullick SH, Ghosh A, Dasgupta D, Kundu PK. 2021. Comparative study between step and sinusoidal temperature profiles during natural

convection inside a square enclosure heated from bottom. In Proceedings of the 48th National Conference on Fluid Mechanics and Fluid Power.

14. Mondal PK, Gaikwad H, Kundu PK, Wongwises S. 2017. Effect of thermal asymmetries on the entropy generation analysis of a variable viscosity Couette–Poiseuille flow. *Proc Inst Mech Eng Part E J Proc Mech Eng* 231(5): 1011-1024. https://doi.org/10.1177/0954408916688234
15. Mullick SH, Kaushik P, Mondal PK, Kundu PK. 2019. Entropy generation in a viscoelastic fluid squeezed and extruded between two parallel plates. In Proceedings of the 25th National and 3rd International ISHMT-ASTFE Heat and Mass Transfer Conference, pp 581-585. https://doi.org/10.1615/IHMTC-2019.980
16. Corcione M. 2003. Effects of the thermal boundary conditions at the sidewalls upon natural convection in rectangular enclosures heated from below and cooled from above. *Int J Therm Sci* 42(2): 199-208. https://doi.org/10.1016/S1290-0729(02)00019-4
17. Basak T, Roy S, Balakrishnan AR. 2006. Effects of thermal boundary conditions on natural convection flows within a square cavity. *Int J Heat Mass Transf* 49(23-24): 4525-4535. https://doi.org/10.1016/j.ijheatmasstransfer.2006.05.015
18. Akterian SG, Fikiin KA. 1994. Numerical simulation of unsteady heat conduction in arbitrary shaped canned foods during sterilization processes. *J Food Eng* 21(3): 343-354. https://doi.org/10.1016/0260-8774(94)90078-7
19. Paroncini M, Corvaro F. 2009. Natural convection in a square enclosure with a hot source. *Int J Therm Sci* 48(9): 1683-1695. https://doi.org/10.1016/j.ijthermalsci.2009.02.005
20. Chen TH, Chen LY. 2007. Study of buoyancy-induced flows subjected to partially heated sources on the left and bottom walls in a square enclosure. *Int J Therm Sci* 46(12): 1219-1231. https://doi.org/10.1016/j.ijthermalsci.2006.11.021
21. Cianfrini C, Corcione M, Dell'Omo PP. 2005. Natural convection in tilted square cavities with differentially heated opposite walls. *Int J Therm Sci* 44(5): 441-451. https://doi.org/10.1016/j.ijthermalsci.2004.11.007
22. Corcione M, Habib E. 2010. Buoyant heat transport in fluids across tilted square cavities discretely heated at one side. *Int J Therm Sci* 49(5): 797-808. https://doi.org/10.1016/j.ijthermalsci.2009.11.012
23. Varol Y, Oztop HF, Pop I. 2009. Natural convection in right-angle porous trapezoidal enclosure partially cooled from inclined wall. *Int Commun Heat Mass Transf* 36(1): 6-15. https://doi.org/10.1016/j.icheatmasstransfer.2008.09.010
24. Bejan A. 2013. Convection Heat Transfer. John Wiley & Sons.
25. Patankar S. 2018. Numerical Heat Transfer and Fluid Flow. CRC Press, Boca Raton.
26. Dutta S, Goswami N, Pati S, Biswas AK. 2021. Natural convection heat transfer and entropy generation in a porous rhombic enclosure: influence of non-uniform heating. *J Therm Anal Calorim* 144: 1493-1515. https://doi.org/10.1007/s10973-020-09634-7
27. Beckermann C, Viskanta R, Ramadhyani S. 1986. A numerical study of non-Darcian natural convection in a vertical enclosure filled with a porous medium. *Numer Heat Transf* 10(6): 557-570. https://doi.org/10.1080/10407788608913535
28. Dutta S, Biswas AK, Pati S. 2017. Effects of non-uniform heating on Natural convection within rhombic enclosures: a numerical study. In Proceedings of the 24th National and 2nd International ISHMT-ASTFE Heat and Mass Transfer Conference, pp 1339-1347. https://doi.org/10.1615/IHMTC-2017.1850
29. Hossain MZ, Floryan JM. 2015. Natural convection in a horizontal fluid layer periodically heated from above and below. *Phys Rev E* 92(2): 023015. https://doi.org/10.1103/PhysRevE.92.023015